Pulsed Electron Paramagnetic Resonance Studies of the Lysine 2,3-Aminomutase Substrate Radical: Evidence for Participation of Pyridoxal 5′-Phosphate in a Radical Rearrangement†

Marcus D. Ballinger,‡ Perry A. Frey,* and George H. Reed*

Institute for Enzyme Research, Graduate School, and Department of Biochemistry, College of Agricultural and Life Sciences, University of Wisconsin—Madison, Madison, Wisconsin 53705

Russell LoBrutto*

Department of Botany, Arizona State University, Tempe, Arizona 85287-1601

Received May 8, 1995®

ABSTRACT: The role of pyridoxal 5′-phosphate (PLP) in the radical-mediated amino group migration catalyzed by lysine 2,3-aminomutase from *Clostridia* SB4 has been investigated by electron spin echo envelope modulation (ESEEM) spectroscopy. This pulsed electron paramagnetic resonance (EPR) method was used to estimate the distance between the unpaired electron in the α-radical of β-lysine, a steady-state intermediate in the reaction, and deuterium at the C4′ position of the cofactor, PLP. [4′-^{2}H]PLP was synthesized and exchanged into the enzyme. The steady-state radical was generated in the labeled samples and in samples with unlabeled PLP by addition of L-lysine·H_2SO_4 to activated enzyme. ESEEM spectra of the samples prepared with [4′-^{2}H]PLP exhibited distinctive low-frequency modulations that were not present in spectra of matched samples with unlabeled PLP. Fourier transformation of the modulations yielded a prominent doublet signal centered about the Larmor frequency of deuterium. The magnitude of the doublet splitting of the ^{2}H ESEEM signal exhibited angle selection across the CW EPR powder pattern. The observed angle selection, as well as simulation of the time domain spectra, indicated that the doublet splitting was due to the combined effects of the ^{2}H hyperfine and nuclear quadrupole interactions. The influences of the quadrupole interaction and of isotropic and dipolar hyperfine interactions were explored by simulations of the ESEEM spectra. The analysis indicates a distance of <3.5 Å between the ^{2}H at C4′ of PLP and the radical center at Cα lysine. The data are most compatible with an aldimine linkage between PLP and the β-nitrogen of β-lysine. These data support the proposed radical rearrangement mechanism, wherein PLP promotes the reaction by formation of an aldimine linkage to the migrating nitrogen.

The classical role of the coenzyme pyridoxal 5′-phosphate (PLP)[1] is to stabilize carbanionic intermediates in enzymatic reactions (Metzler et al., 1954). When PLP is bonded in an aldimine linkage to amino acid substrates, it serves as an "electron sink" that facilitates delocalization of negative charge developed on the substrate α, β, or γ carbon atoms of intermediates in transaminations, racemizations, decarboxylations, eliminations, and substitutions (Walsh, 1978; Bruice & Benkovic, 1966). In another class of PLP-dependent reactions, the 1,2-amino group migrations catalyzed by aminomutases, PLP has been postulated to participate in the isomerization of organic radical intermediates (Frey et al., 1990; Frey, 1990; Moss & Frey, 1987). Thus far, evidence for this expanded role of PLP has been indirect, namely, a specific cofactor requirement for PLP exhibited by aminomutases for which radical intermediates have been implicated or might be expected. The conjecture that PLP can assist in free radical-mediated rearrangements is reinforced by a chemical model study in which an analogous arylaldimine linkage supports the same type of radical rearrangement of an amino acid ester (Han & Frey, 1990).

The PLP-dependent enzyme lysine 2,3-aminomutase catalyzes the first step in lysine metabolism in *Clostridia*, the conversion of L-α-lysine to L-β-lysine (Chirpich et al., 1970; Stadtman, 1973). The purified enzyme requires activation by a prolonged incubation with a sulfhydryl reductant and subsequent addition of another cofactor, *S*-adenosylmethionine (Chirpich et al., 1970; Petrovich et al., 1991, 1992). The participation of the adenosyl-5′-methylene group of *S*-adenosylmethionine in the hydrogen-transfer process (Moss & Frey, 1987; Baraniak et al., 1989) and the EPR detection and subsequent characterization of an intermediate, the α-radical of β-lysine (Ballinger et al., 1992a; 1992b), are consistent with the mechanism shown in Scheme 1. Migration of the α-amino group to the β-carbon, to produce the

† This work was supported by Grants DK28607 (P.A.F.) and GM35752 (G.H.R.) from the NIH and by an NRSA Fellowship (M.D.B.) from NIH Training Grant GM08293.

‡ Present address: Department of Protein Engineering, Genentech Inc., S. San Francisco, CA 94080.

® Abstract published in *Advance ACS Abstracts,* July 15, 1995.

[1] Abbreviations: PLP, pyridoxal 5′-phosphate; EPR, electron paramagnetic resonance; ESE, electron spin echo; ESEEM, electron spin echo envelope modulation; ENDOR, electron nuclear double resonance; CW, continuous wave; NMR, nuclear magnetic resonance; S/N, signal-to-noise.

[2] Corrections due to uncertainties in the extent of exchange of labeled PLP enter into the distance calculation with a sixth-root dependence, and their combined effects on the distance are on the order of 10%.

[3] The distance represents an r^{-6} weighted average distance between the unpaired electron and the ^{2}H. Previous studies (Ballinger et al., 1992b) indicate that the α-radical has ~80% spin density in a p_z orbital on Cα. The remainder of the spin density is likely in the π orbitals of the adjacent carboxylate group.

0006-2960/95/0434-10086$09.00/0

Scheme 1

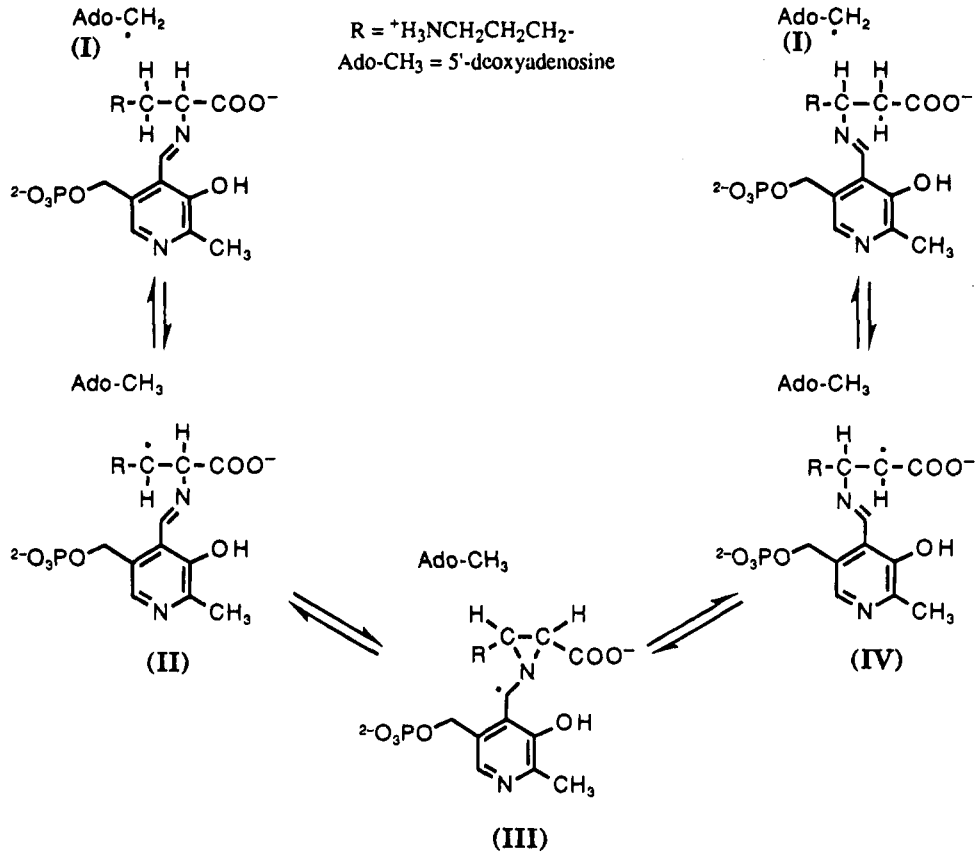

α-radical of β-lysine-PLP (**IV**), is thought to proceed through an azocyclopropylcarbinyl radical (**III**). In this proposed scheme, the aldimine linkage between lysine and PLP is essential to the mechanism. PLP could also contribute to the stability of the azocyclopropylcarbinyl radical (**III**) by allowing partial delocalization of the unpaired electron into the π system of its pyridine ring.

Experimental evidence for the attachment of the substrate to PLP at the active site of lysine 2,3-aminomutase has, however, been elusive. Attempts to inhibit the reaction by reduction of the imine linkage with $NaBH_4$ have been unsuccessful (P. A. Frey, K. B. Song, and J. R. Burke, unpublished observations). Furthermore, the near-UV to visible region of the optical spectrum of the enzyme is dominated by a strong absorbance which arises from the iron−sulfur centers associated with the protein. This strong absorbance masks characteristic electronic transitions that might be associated with the presumed PLP aldimine adduct.

In the steady state of the reaction, the α-radical of β-lysine (**IV**), which follows the azocyclopropylcarbinyl radical intermediate in Scheme 1, appears at concentrations that allow detection and characterization by conventional CW EPR (Ballinger et al., 1992a,b). The CW EPR spectrum of this intermediate, however, does not provide information on the state of protonation or the chemical form of the β-nitrogen of **IV**. Thus, earlier EPR experiments did not implicate PLP in the structure of the substrate radical intermediate (Ballinger et al., 1992b).

Weak, long-range, hyperfine interactions in paramagnetic species are frequently detectable by the pulsed ESE method of ESEEM spectroscopy (Mims, 1972a; Norris et al., 1980; Mims & Peisach, 1981). In these EPR measurements, nuclear spins that are weakly coupled to the unpaired electron spin can produce modulations in the amplitudes of electron spin echoes. The frequencies of these modulations are analogous to the classical ENDOR frequencies of the coupled nuclear spins, and a frequency spectrum is obtained by Fourier transformation of the amplitude modulations. The magnetic properties of deuterium make it an especially sensitive nucleus for ESEEM detection at X-band EPR frequencies. ESEEM spectroscopy has been used previously to investigate the radical signal in ethanolamine ammonia lyase (Tan et al., 1986) and more recently to investigate the radical associated with an inhibited form of ribonucleotide reductase (Salowe et al., 1993). In the present work, ESEEM spectroscopy and [4′-^{2}H]PLP have been used to determine the proximity of PLP to the unpaired electron in the α-radical of β-lysine (**IV**) produced in the lysine aminomutase reaction.

EXPERIMENTAL PROCEDURES

Materials. Lysine 2,3-aminomutase was purified from *Clostridium* SB4 and assayed using procedures described previously (Moss & Frey, 1987; Petrovich et al., 1991). NaB^3H_4 (100 mCi/mmol) was obtained from Amersham. NaB^2H_4 (98% atom ^{2}H) was from Aldrich. PLP was from Sigma. MnO_2 was prepared according to a published procedure (Lui et al., 1981). L-lysine·H_2SO_4 was prepared from L-lysine·HCl by ion-exchange chromatography. Lysine·HCl dissolved in 10 mM HCl was loaded on a column of Dowex 50W-X8, which was then washed with water and eluted with 1 M ammonia. Fractions containing lysine were pooled, evaporated to a syrup, redissolved in a small volume of water, and combined with 1 equiv of H_2SO_4. Lyophilization yielded L-lysine·H_2SO_4. Stock solutions of L-lysine·H_2SO_4 used in enzymatic reactions were adjusted to pH 8 by addition of 10 M NaOH.

Synthesis of [4′-^{3}H]PLP and [4′-^{2}H]PLP. [4′-^{3}H]PLP was prepared by following the published procedure (Stock et al., 1966) using the following modifications. The pH of the PLP solution prior to reduction by $NaBH_4$ was adjusted by addition of NaOH in place of $NaHCO_3$, and HCl was used in place of $HClO_4$ to acidify the solution for subsequent oxidation by MnO_2. The pH of the reaction mixture after reoxidation by MnO_2 was adjusted to ~8 by addition of 3 M NaOH, and the unreacted MnO_2 was removed by filtration. [4′-^{3}H]PLP and unlabeled PLP were collected in a single fraction from the Dowex 1-X8 column, and the solvent was removed by lyophilization, yielding [4′-^{3}H]PLP with a specific radioactivity of 7.2 mCi/mmol. [4′-^{2}H]PLP was obtained similarly by use of NaB^2H_4. Two cycles of reduction/oxidation were performed to maximize the incorporation of deuterium. Integrals of the ^{1}H NMR signal at δ = 10.2 ppm showed approximately 94% ^{2}H enrichment specifically at the 4′-position.

Exchange of Enzyme-Bound PLP. Lysine 2,3-aminomutase in standard isolation buffer (30 mM Tris·H_2SO_4 at pH 8.0, 1 mM dithiothreitol, 0.1 mM L-lysine·HCl, and 0.01 mM PLP) was combined in a 500-μL microfuge tube with reductive incubation components to give a 150-μL solution containing final concentrations of 0.12 M Tris·H_2SO_4 at pH 8.0, 0.6 mM sodium dithionite, 20 mM PLP or [4′-^{3}H]PLP (7.2 mCi mmol^{-1}), 0.8 mM ferric ammonium citrate, 6.3 mM dihydrolipoic acid, and 70 μM oligomeric enzyme. The solution was incubated in this activation solution at 37 °C for 5.5 h. To assay enzyme activity, a small volume (~10 μL) of the activation mixture was removed and added to a solution of substrate to give final concentrations of 80 mM Tris·H_2SO_4 at pH 8.0, 2.0 mM sodium dithionite, 150 mM [^{14}C]lysine·H_2SO_4, 1.3 mM *S*-adenosylmethionine, and 30 μM enzyme. The assay reaction was quenched at 30 s with 50 μL of 0.2 M formic acid, and α- and β-lysine products were separated and quantitated according to the published procedure (Chirpich et al., 1970). The remainder of the reductive incubation solution was chromatographed on a 1.5 × 18 cm column of Sephadex G-25 to separate exogenous PLP from the enzyme. The column was equilibrated and eluted with a buffer containing 30 mM Tris·H_2SO_4 at pH 7.5, 1 mM dithiothreitol, and 0.1 mM lysine·HCl. Fractions were analyzed for absorbance at 280 and 388 nm and for radioactivity by scintillation counting of small aliquots. Fractions in which the greater part of the enzyme emerged were analyzed for protein concentration by the method of Lowry (Cooper, 1977). The PLP content of these fractions was assayed by the procedure of Wada and Snell (Wada & Snell, 1961) following deproteinization by treatment with 1% SDS for 10 min, acidification to 0.1 M in HCl, and centrifugation. The 410-nm absorbances from PLP−phenylhydrazone adducts were compared to a standard curve to determine the PLP content. The extent of PLP exchange was calculated by dividing the specific radioactivity of the enzyme-bound [4′-^{3}H]PLP by that of the original [4′-^{3}H]PLP.

Preparation of Samples for EPR and ESEEM. In order to compare the results obtained using different salts of lysine, samples were prepared as described previously (Ballinger et al., 1992a), except that less Tris·HCl (40 mM), sodium dithionite (2.3 mM), and lysine (150 mM) were used in the reactions to lower the ionic strength.

Samples of enzyme with either [4′-^{2}H]PLP or unlabeled PLP (control samples) were reductively incubated as described for the radiochemical experiments above. Reduced enzyme (100 μL) was then added to reaction components to give concentrations of 80 mM Tris·H_2SO_4 at pH 8.0, 2.3 mM sodium dithionite, 150 mM L-lysine·H_2SO_4, and 1.3 mM *S*-adenosylmethionine, in addition to other components carried over from the reductive incubation, in a final volume of 230 μL. Solutions were mixed, transferred to EPR tubes, and frozen in liquid N_2 within 20−30 s. All of these steps were carried out on samples contained within a Coy anaerobic chamber.

EPR and ESEEM Measurements. CW EPR spectra were recorded on a Varian E-3 spectrometer at 77 K using a liquid N_2 immersion Dewar as described previously (Ballinger et al., 1992b). Three-pulse (stimulated echo) ESEEM measurements were made using a lab-built, pulsed EPR spectrometer (LoBrutto et al., 1986). A two-loop, two-gap resonator (Froncisz & Hyde, 1982) made of copper foil was mounted on the hourglass sample tube holder of an ADP Cryogenics LTR flow cryostat. A traveling wave tube microwave power amplifier with a nominal output of 50 W was combined with the resonator to produce $\pi/2$ pulses of 12-ns duration. ESEEM measurements were performed at 9.0 GHz. A sample temperature of 12 K was maintained throughout. At this temperature, the pulse repetition rate of 3 kHz allowed sufficient time between pulse trains for the spin populations to reequilibrate. Although measurements at 4.2 K produced more intense spin echoes, the need to reduce the repetition rate to avoid saturation resulted in a net loss of S/N in the signal-averaged spectrum. In each spectrum, a τ-value (time between pulses 1 and 2) of 220 ns was employed. The independent variable in time-domain spectra is τ', the time between pulses 1 and 3 ($\tau' = T + \tau$, where T is the variable time between pulses 2 and 3). Frequency-domain presentations of ESEEM spectra were obtained by Fourier transformation of time-domain spectra. Prior to Fourier transformation, the time-domain data were fitted to a single-exponential function, which was then subtracted from the data. The initial portions of the spectra were removed to eliminate dead time following the pulse train (this treatment was applied to simulated ESEEM spectra as well). The spectra were apodized, transformed, and displayed in modulus form.

Simulation of Time- and Frequency-Domain ESEEM Spectra. The time record of three-pulse (stimulated echo) modulations due to the nuclear spin of ^{2}H (I = 1) was simulated by use of a program generously supplied by the Biotechnology Resource in Pulsed EPR at the Albert Einstein College of Medicine, Bronx, New York. This program incorporates the formalism of Mims (1972b,c) for calculation of stimulated echo ESEEM spectra, as well as the angle-selection scheme of Hurst et al. (1985). A detailed description of the simulation procedure is given by Cornelius et al. (1990). In the present case, the strong and highly anisotropic α proton hyperfine coupling largely determines which molecular orientations are selected at a given magnetic field setting. The principal axes of the ^{1}Hα hyperfine coupling tensor (Chart 1) serve as the reference axis system, because the g factor is nearly isotropic. The effects of other, smaller nuclear hyperfine couplings (except for ^{2}H) are not included explicitly in the calculation of the ESEEM spectrum, but are accounted for by application of a line-shape function (Cornelius et al., 1990). As a direct measurement of the ^{2}H nuclear quadrupole parameter, e^2Qq, was not available, a range of values from 0.16 to 0.33 MHz was explored.

Euler angles describing the orientations of the ^{2}H hyperfine and quadrupole tensors with respect to the reference axes

Chart 1

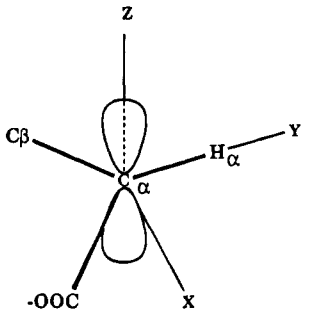

were calculated according to the conventions of Rose (1957). The Euler angles are dependent upon the torsion angle defined by the axis of the p_z orbital of Cα and atoms Cα, Cβ, and Nβ. This angle has been determined by detailed simulations of CW spectra of the Cα-based radical to be in the 7−10° range (Ballinger et al., 1992b). The only remaining degree of freedom that affects the Euler angles is the rotation angle about the Cβ−Nβ bond. Rotation about this bond determines the distance, r, and for a given value of r there are two sets of Euler angles.

For quantitation of modulation depths relative to the overall spin echo amplitude, the modulation depth parameter d (Mims et al., 1990) was used. For depths in a one-cycle interval encompassing two troughs and the intervening peak, d is defined as

$$d = 1 - \frac{[y(\text{trough } n) + y(\text{trough } n+2)]}{2y(\text{peak } n+1)} \qquad (1)$$

where n is the index number of the peak or trough counted serially, beginning with $n = 0$ for the peak in the cosine modulation function which occurs at $\tau' = 0$. In the present case, troughs 3 and 5 and peak 4, representing the first full detectable cycle in the ^2H modulation data, were used. In order to reduce the influence of noise in choosing y values for use in eq 1, the first two observable cycles of experimental data were fitted to an exponentially decaying cosine curve by an interative least-squares procedure (inset, Figure 2a). The y values of the cosine curve at the appropriate times τ' were then used to obtain d.

Before comparing experimental with theoretical values of d, the experimental value had to be corrected for the estimated fraction, j, of exchange of the isotopically labeled PLP into the enzyme, because the simulations are based on 100% abundance of ^2H. Because the modulation depth should be a simple linear function of j, the experimental value of d was simply divided by j to obtain the corrected modulation depth, d'.

It must be emphasized that, although eq 1 was used to calculate the depth parameter from both experimental and simulated time-domain ESEEM spectra, the depth parameter was not used to calculate distances directly, as suggested by Mims et al. (1990). In order to avoid potential inaccuracies due to a nonzero isotropic (scalar) component of the deuterium hyperfine coupling, simulations were used to analyze the experimental spectra. The depth parameter d was used in this context simply to facilitate the comparison between experimental and simulated modulation depths.

RESULTS

Effects of Sulfate versus Chloride Ions on the Yields of the Product Radical. Samples of the steady-state radical prepared as described previously with L-lysine•2HCl as the substrate yielded radical concentrations ~10% of the protein hexamer concentration, or 4−5 μM, (Ballinger et al., 1992a). These samples gave electron spin echoes that were too weak to produce observable ESEEM. Substantial increases (3−4-fold) in radical concentration were, however, obtained when L-lysine•H_2SO_4 was used as a substrate. Because the enzyme activity in solution is insensitive to changes in counter ions, the deleterious effect of chloride on the yield of radical appears to be exerted during the freezing of the samples. With L-lysine•H_2SO_4 as the substrate, a sample containing 47 μM oligomeric enzyme (specific activity under conditions of EPR sampling = 11.5 IU mg^{-1}) yielded a concentration of radical of 26 μM. Replacement of chloride by sulfate, together with use of a more concentrated solution of enzyme, provided a dramatic increase in S/N of the CW and ESE spectra.

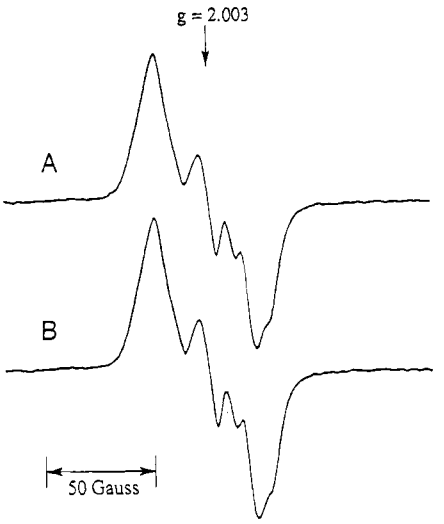

FIGURE 1: EPR spectra (77 K) of the steady-state reaction mixtures of lysine 2,3-aminomutase after either unlabeled PLP (A) or [4′-^{2}H]PLP (B) was exchanged into the protein. The samples contained enzyme (43 μM oligomer concentration) after 5.5 h of reductive incubation/PLP exchange (see Experimental Procedures), Tris/H_2SO_4 at pH 8.0 (80 mM), sodium dithionite (2.3 mM), *S*-adenosylmethionine (1.3 mM), and L-lysine•H_2SO_4 (150 mM). The spectra were acquired from single scans, with a microwave power of 2.5 mW, a modulation amplitude of 2.5 G, and a microwave frequency of 9.044 GHz.

Exchange of Enzyme-Bound PLP. In order to generate enzyme containing [4′-^{2}H]PLP, a procedure for partial exchange of the cofactor was devised. The requirement for ~0.4 mM PLP in the standard reductive incubation of lysine 2,3-aminomutase for maximal activation implied that PLP binds reversibly to the protein and also suggested that exchange during the incubation should be feasible. To assess the ability of the enzyme-bound PLP to exchange with free PLP, the reductive incubation phase of the standard assay was carried out in the presence of a 50-fold molar excess (with respect to the subunit concentration of enzyme) of [4′-^{3}H]PLP. After separation of free [4′-^{3}H]PLP at the conclusion of the incubation, the specific radioactivity of enzyme-associated PLP indicated 46 and 64% exchange in two experiments. Under these conditions, the enzyme did not bind excess PLP. Assays of PLP content gave 5.5 ± 0.3 PLP/hexamer, a value in good agreement with previous studies (Song & Frey, 1991). In addition, excess PLP did not affect the enzymatic activity or production of the radical intermediate.

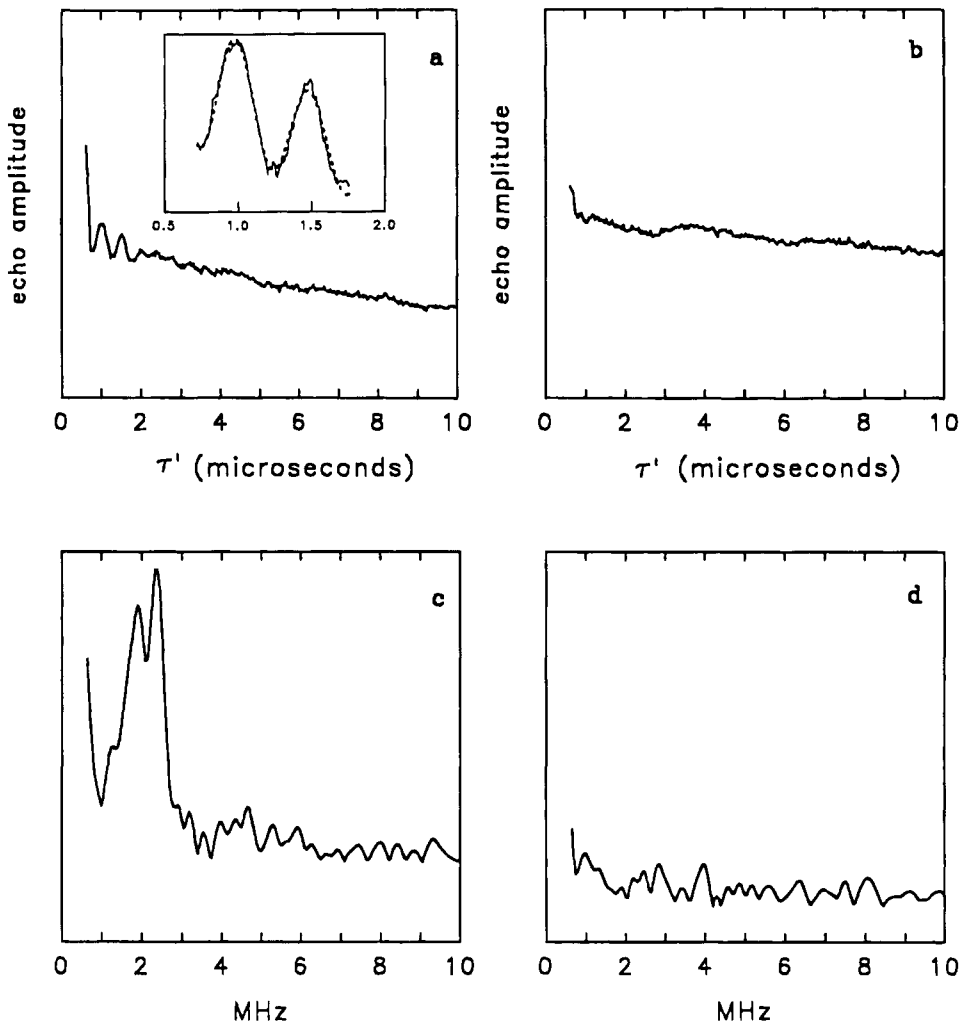

FIGURE 2: Time and frequency domain ESEEM spectra of the steady-state radical intermediate in lysine 2,3-aminomutase generated using the samples whose CW spectra are shown in Figure 1: (a and c) [4′-^{2}H]PLP or (b and d) unlabeled PLP. The inset to (a) shows an expansion of the first two (detected) cycles of ^{2}H modulation. The three troughs are indexed as $m = 3$, 5, and 7, while the two peaks carry indices $m = 4$ and 6. The smooth curve is a damped cosine function superimposed upon a decaying exponential and fitted to the experimental data. Experimental conditions: $H_0 = 3200$ G; $\nu_e = 9.0126$ GHz; $\tau = 0.220$ μs; $T = 12$ K; repetition rate = 3.05 kHz. Each time point represents the sum of amplitudes of ~5700 spin echoes.

Detection of 4′-^{2}H Hyperfine Coupling by ESEEM Spectroscopy. CW EPR spectra from unlabeled samples and from samples in which there was exchange of [4′-^{2}H]PLP into the enzyme were virtually identical (Figure 1). Figure 2 shows three-pulse ESEEM spectra obtained from these samples. The time-domain spectrum of the sample containing [4′-^{2}H]PLP (Figure 2a) exhibits low-frequency modulations that are absent in the spectrum of the sample with unlabeled PLP (Figure 2b). The corresponding frequency-domain spectrum (Figure 2c, solid curve) of the sample prepared with [4′-^{2}H]PLP shows a split peak centered at the ^{2}H Larmor frequency of 2.1 MHz. This signal is assigned to ^{2}H by virtue of the absence of an analogous signal in the spectrum of the unlabeled control (Figure 2d) and by its characteristic frequency. Observation of ^{2}H modulations in Figure 2a immediately demonstrates that the ^{2}H is within a radius of ~6 Å of the unpaired spin at C_α. The split ^{2}H signal in the frequency-domain spectrum (Figure 2c, solid curve) suggests a strong interaction and, therefore, a shorter distance.

The absence of low-frequency modulations in the ESEEM spectra due to ^{14}N is consistent with the proposed structure of the radical and with the CW EPR results (Ballinger et al., 1992b). The β-nitrogen of the α radical couples strongly ($a^{14}_N = 23$ MHz) to the unpaired electron, and such strongly coupled nuclei do not normally give rise to ESEEM (Mims & Peisach, 1981). The other nitrogens in the molecule are evidently too far from the unpaired electron to give detectable modulations.

Analysis of Spin-Echo Modulations in the Time and Frequency Domains. Initial ESEEM measurements revealed that splitting of the doublet signal was more pronounced when the magnetic field corresponded to the low-field edge of the CW powder spectrum of the radical. The β-nitrogen of the radical harbors ~1% spin density (Ballinger et al., 1992b). A scalar contribution to the hyperfine splitting of the ^{2}H at C4′ of plus or minus a few tenths MHz might be propogated, by polarization through the proposed linkage between C4′ and the β-nitrogen. Chemically reasonable models that allow appreciable scalar hyperfine splitting, however, also place the ^{2}H within 3−4 Å of the center of the unpaired spin, and at this range of distances, the dipolar hyperfine splitting will be also be significant. ESEEM frequency spectra taken at three field settings corresponding to the low-, middle-, and high-field positions within the CW absorption spectrum of the radical are shown in Figure 3. Splitting of the ^{2}H signal is most prominent at the low- and high-field edges of the CW spectrum, and it is less resolved

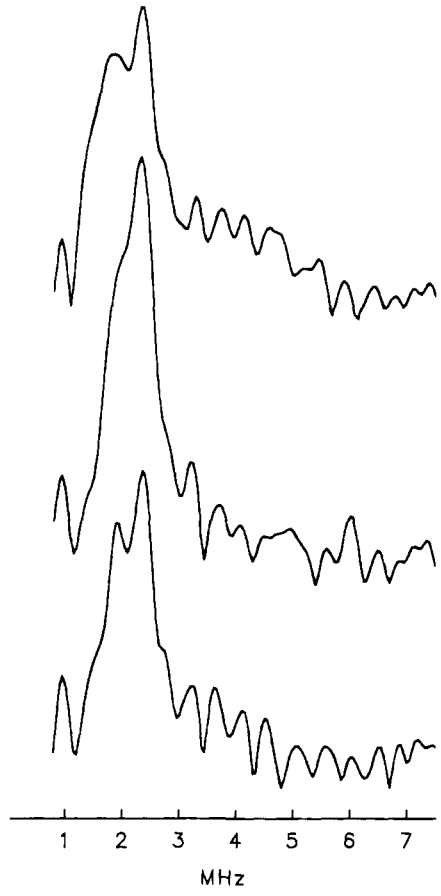

FIGURE 3: Frequency domain ESEEM spectra obtained from the same sample as in Figure 2a,c), and under matching conditions, except that H_0 = 3183 (top); 3205 (middle), and 3225 G (bottom).

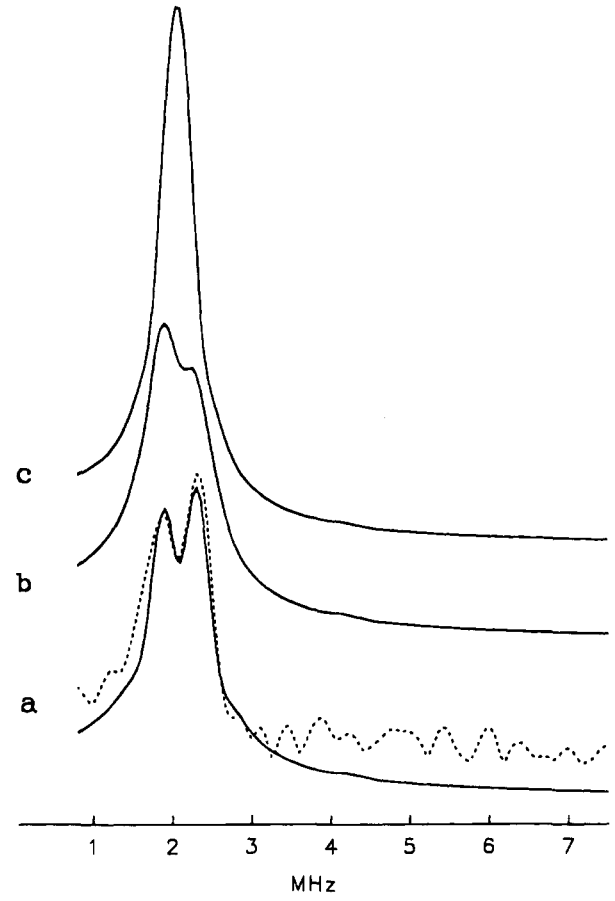

FIGURE 4: Simulated frequency domain ESEEM spectra: (a) best fit obtained to experimental spectrum (latter shown as dashed line). Electron spin Hamiltonian parameters used in the simulations: g_{xx}, g_{yy}, g_{zz} = (2.0021, 2.0037, 2.0043) MHz; α-proton hyperfine tensor, A_{xx}, A_{yy}, A_{zz} = (−60.8, −28.3, −91.3) MHz; Euler angles, $\alpha = \beta = \gamma = 0°$. Spin Hamiltonian parameters for the ^{2}H: ^{2}H hyperfine tensor, A_{xx}, A_{yy}, A_{zz} = (−0.27, −0.27, 0.84) MHz (a^2_H = 0.10 MHz); Euler angles, $\alpha = 0°$, $\beta = -135°$, $\gamma = -170°$. Quadrupolar parameters: e^2Qq = 0.33 MHz; η = 0.04; Euler angles, $\alpha = 145°$, $\beta = -75°$, $\gamma = -110°$. (b) The same as (a) except that the quadrupolar Euler angles are all set equal to 0°. (c) The same as (a) except that $e^2Qq = 0$.

near the center where S/N is highest. The angle selection that is reflected in the ESEEM spectra is elaborated because of anisotropy in the α-proton hyperfine splitting (Ballinger et al., 1992).

The influences of the dipolar and scalar hyperfine interactions and of the nuclear quadrupole interaction of ^{2}H on the ESEEM spectra were explored by simulations. A significant scalar coupling requires a through-bond connection between the unpaired electron on the α-carbon of the β-lysine fragment and the cofactor, PLP, so a model of the putative PLP−β-lysine adduct was used to guide the analysis. Although the fits to the experimental spectra may not be entirely unique, given the number of geometric and magnetic parameters involved, difficulties encountered in reproducing the basic characteristics of the spectra lend confidence to the analysis.

Effect of the Deuterium Nuclear Quadrupole Interaction on the ESEEM Spectrum. Splittings arising from nuclear hyperfine or quadrupole interactions are difficult to differentiate in some cases (Kevan, 1979). In order to gauge the relative influence of the latter upon the ESEEM spectrum of Figure 2, a series of simulations was performed (Figure 4). First, a simulation based upon a best fit set of parameters was calculated, using, for example, e^2Qq = 0.33 MHz (Figure 4a); the validity of the other parameters used to achieve this fit was tested in other simulations. Next, the Euler angles for the quadrupole interaction were assigned arbitrary values of zero, rather than the values based upon the model of the proposed PLP adduct to the lysine Cα radical. The result was an ESEEM frequency spectrum with a reduced doublet splitting and with reversal in relative amplitudes of the two peaks (Figure 4b). Finally, the simulation of Figure 4c was derived from the best fit spectrum (Figure 4a) by setting e^2Qq equal to zero. The result was that virtually all of the splitting was lost, and the peak became narrower and more intense. These observations indicate that a major portion of the doublet splitting may arise from the ^{2}H quadrupole coupling and that the dependence of the splitting on the position within the CW absorption envelope, demonstrated in Figure 3, is probably attributable in large part to the anisotropy of this quadrupole interaction. Equivalent fits (not shown) to the data are obtained using e^2Qq = 0.16 MHz by adjusting the isotropic component of the ^{2}H hyperfine coupling to −0.05 MHz.

Effect of a^2_H on the ESEEM Spectra. The influences of isotropic coupling, a^2_H, on the ESEEM spectra were more readily visualized in the time domain. Figure 5 shows six simulated ESE envelopes, calculated using the best fit parameters, but with varying values of a^2_H. In general, the simulated modulations tend to decay more rapidly than those in the experimental spectrum (Figure 5c, immediately below simulation) if a nonzero $|a^2_H| > 0.1$ MHz is used (all signs of hyperfine couplings are relative only). This trend is most conspicuous in simulations with negative values of a^2_H for

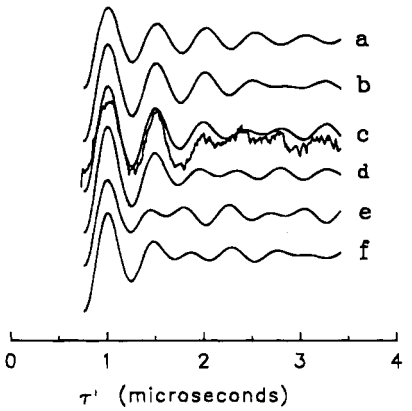

FIGURE 5: Simulated time domain ESEEM spectra. Parameters are the same as in figure 4a except for the values of a^2_H. For spectra a through f, a^2_H = 0.30, 0.20, 0.10, 0.0, −0.10, and −0.20 MHz, respectively. The third value (a^2_H = 0.10 MHz) yields the best fit to the experimental data, which are shown for comparison directly below simulation c.

which the depth of the second cycle, in particular, becomes substantially shallower than the experimental data when $a^2_H \leq -0.10$ MHz. For positive values of a^2_H, the modulations do not decay quite as quickly as for negative values. Only a single modulation period is, however, evident at 0.30 MHz, and the modulation phases in the later cycles differ from those of the experimental spectra. The simulations shown are meant to be representative rather than inclusive; many other values of a^2_H were tried, in combination with a range of r values between 3.0 and 4.1 Å. The data are clearly best approximated by $-0.1 \leq a^2_H \leq 0.1$ MHz, and isotropic hyperfine coupling is not the major interaction responsible for the doublet splitting.

Effect of Electron−Deuteron Distance r on the ESEEM Spectrum. As is well known in ESEEM (Mims et al., 1990), the depth of a given cycle of modulation relative to the total echo amplitude is proportional to the inverse sixth power of the distance. The depth parameter, d, corresponding to the first full observable modulation cycle, was measured for both simulated and experimental spectra. Figure 6 shows the results of five simulations corresponding to r = 4.0, 3.8, 3.5, 3.2, and 3.0 Å. The simulated depths, d, were 0.03, 0.04, 0.05, 0.08, and 0.12 Å, respectively. The experimental modulation depth, corrected for extent of exchange of labeled PLP, for this same cycle fell in the range of 0.10−0.14 assuming 64% and 46% exchange, respectively. Thus, the distances, 3.0 Å < r < 3.5 Å (the latter being a generous upper limit), are most compatible with the modulation depths.

DISCUSSION

The observation of spin coupling between the product radical (**IV** in Scheme 1) in the lysine 2,3-aminomutase reaction and ^{2}H in [4′-^{2}H]PLP provides experimental evidence for proximity of the cofactor and substrate radical at the active site of the enzyme. A detectable scalar component in the coupling requires a direct chemical linkage between the β-N and C4′ of the cofactor. At this point, while simulations point toward a small isotropic component of the coupling, the analysis provides no direct evidence for a scalar contribution to the hyperfine interaction comparable to the observed splitting in the ^{2}H ESEEM spectra. Distances between the Cα and the 4′-^{2}H of PLP of <3.5 Å are, however, compatible with the proposed aldimine linkage between C4′ of PLP and the β-N of the radical. Moreover,

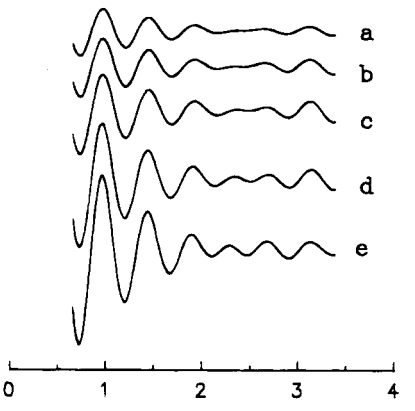

FIGURE 6: Simulated time domain ESEEM spectra, using the same parameters as in Figures 4a and 5c, except that the principal values of the ^{2}H hyperfine tensor and the Euler angles for the ^{2}H hyperfine and quadrupole tensors have been adjusted to reflect variation in r, the electron−^{2}H distance. The distances assumed and the corresponding parameters are as follows: (a) r = 4.0 Å; ^{2}H hyperfine parameters, A_{xx}, A_{yy}, A_{zz} = (−0.09, −0.09, 0.48) MHz; Euler angles, α = 0°, β = −110°, γ = −210°; quadrupolar Euler angles, α = 145°, β = −40°, γ = −210°; (b) r = 3.8 Å; ^{2}H hyperfine parameters, A_{xx}, A_{yy}, A_{zz} = (−0.12, −0.12, 0.54) MHz, Euler angles, α = 0°, β = −120°, γ = −190°; quadrupolar Euler angles, α = 145°, β = −45°, γ = −185°; (c) r = 3.5 Å; ^{2}H hyperfine parameters, A_{xx}, A_{yy}, A_{zz} = (−0.18, −0.18, 0.66) MHz, Euler angles, α = 0°, β = −135°, γ = −165°; quadrupolar Euler angles, α = 145°, β = −60°, γ = −155°; (d) r = 3.2 Å; ^{2}H hyperfine parameters, A_{xx}, A_{yy}, A_{zz} = (−0.27, −0.27, 0.84) MHz, Euler angles, α = 0°, β = −135°, γ = −170°; quadrupolar Euler angles, α = 145°, β = −75°, γ = −110°; (e) r = 3.0 Å; ^{2}H hyperfine parameters, A_{xx}, A_{yy}, A_{zz} = (−0.35, −0.35, 1.00) MHz, Euler angles, α = 0°, β = −135°, γ = −140°; quadrupolar Euler angles, α = 145°, β = −50°, γ = −90°.

Chart 2

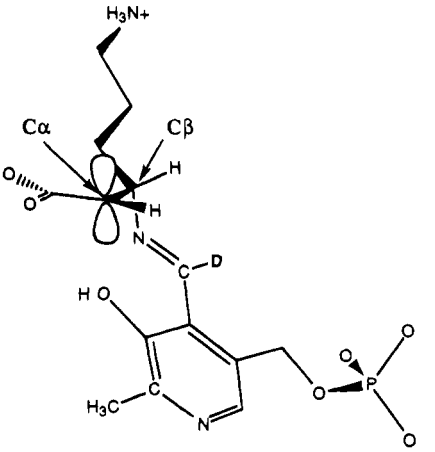

the splitting in the ESEEM spectra is modeled effectively at this distance by the hyperfine and nuclear quadrupole interactions of the C4′-^{2}H. A model of the radical intermediate that incorporates this range of distances and the aldimine linkage is shown in Chart 2.

Although attachment of PLP to the β-amino group is the most reasonable interpretation of the distance measurement, other scenarios cannot be completely ruled out. Molecular models indicate that this distance can be achieved by attachment of PLP to the ε-amino group of the substrate. This alternative structure appears unlikely, however, because the H$_4$′−Cα distance constraint forces unfavorable eclipsing interactions amongst the β-lysine methylene groups. The possibility that PLP is not linked covalently to lysine, but is

approximately 3.2 Å away from Cα of the radical in the active site, seems highly unlikely. An aldimine linkage between PLP and the β-nitrogen, on the other hand, accommodates both the experimentally determined distance constraint and a plausible role for PLP in the enzymatic reaction.

The steady-state (Ballinger et al., 1992b) and pre-steady-state (Ballinger, 1993) concentrations of the azocyclopropylcarbinyl radical (**III** in Scheme 1) are too low to permit EPR detection. Hence, it is not yet possible to determine the extent of unpaired spin delocalization into the π orbitals of the pyridine ring and, thereby, the contributions of such spin delocalization to the stability of this putative intermediate.

The aldimine linkage is a requirement (Han & Frey, 1990) for the radical-mediated reaction outlined in Scheme 1. Alternative mechanisms for the α−β migration of the amino group in radical intermediates are unattractive for lysine 2,3-aminomutase. Such schemes require departure of NH_3 from the β- and α-radicals of lysine, leaving cation radicals that would lack stabilizing substituents such as adjacent hydroxyl groups (Frey, 1990). The present results reinforce the notion that the coenzyme, PLP, facilitates radical-mediated rearrangements and is, therefore, more versatile in its role as a cofactor than has been generally recognized previously.

ACKNOWLEDGMENT

We are grateful to Dr. Christopher Halkides for helpful discussions.

REFERENCES

Aberhart, D. J., Gould, S. J., Lin, T. K., Thiruvengadam, T. K., & Weillor, B. H. (1983) *J. Am. Chem. Soc. 105*, 5461−5470.
Ballinger, M. D. (1993) Ph.D. Thesis, University of Wisconsin−Madison, Madison, WI.
Ballinger, M. D., Reed, G. H., & Frey, P. A. (1992a) *Biochemistry 31*, 949−953.
Ballinger, M. D., Frey, P. A., & Reed, G. H. (1992b) *Biochemistry 31*, 10782−10789.
Baraniak, J., Moss, M. L. & Frey, P. A. (1989) *J. Biol. Chem. 264*, 1357−1360.
Bruice, T. C., & Benkovic, S. J. (1966) in *Bioorganic Mechanisms, Vol. II*, W. A. Benjamin, Inc., New York.
Chirpich, T. P., Zappia, V., Costilow, R. N., & Barker, H. A. (1970) *J. Biol. Chem. 245*, 1778−1789.
Cooper, T. C. (1977) *The Tools of Biochemistry*, pp 53−55, Wiley & Sons, New York.
Cornelius, J. B., McCracken, J., Clarkson, R. B., Belford, R. L., & Peisach, J. (1990) *J. Phys. Chem. 94*, 6977−6982.
Frey, P. A. (1990) *Chem. Rev. 90*, 1343−1357.
Frey, P. A., Moss, M., Petrovich, R. M., & Baraniak, J. (1990) *Ann. N.Y. Acad. Sci. 585*, 368−378.
Froncisz, W., & Hyde, J. S. (1982) *J. Magn. Reson. 47*, 515−521.
Han, O., & Frey, P. A. (1990) *J. Am. Chem. Soc. 112*, 8982−8983.
Hoffman, B. M., DeRose, V. J., Doan, P. E., Gubriel, R. J., Houseman, A. L. P., & Telser, J. (1993) *Biol. Magn. Reson. 13*, 151−218.
Hurst, G. C., Henderson, T. A., & Kreilick, R. W. (1985) *J. Am. Chem. Soc. 107*, 7294−7299.
Kevan, L. (1979) in *Time Domain Electron Spin Resonance* (Kevan, L., & Schwartz, R. N., Eds.) pp 279−341, Wiley, New York.
Lui, A., Minter, R., Lmeng, L., & Li, T. K. (1981) *Anal. Biochem. 112*, 17−22.
LoBrutto, R., Smithers, G. W., Reed, G. H., Orme-Johnson, W. H., Tan, S. L., & Leigh, J. S., Jr. (1986) *Biochemistry 25*, 5654−5660.
Metzler, D. E., Ikawa, M., & Snell, E. E. (1954) *J. Am. Chem. Soc. 76*, 648.
Mims, W. B. (1972a) in *Electron Paramagnetic Resonance* (Geschwind, S., Ed.) pp 263−351, Plenum, New York.
Mims, W. B. (1972b) *Phys. Rev. B5*, 2409−2419.
Mims, W. B. (1972c) *Phys. Rev. B6*, 3543.
Mims, W. B., & Peisach, J. (1981) *Biol. Magn. Reson. 3*, 213−263.
Mims, W. B., Davis, J. L., & Peisach, J. (1990) *J. Magn. Reson. 86*, 273−292.
Moss, M. L., & Frey, P. A. (1987) *J. Biol. Chem. 262*, 14859−14861.
Mustafi, D., Sachleben, J. R., Wells, G. B., & Makinen, M. W. (1992) *J. Am. Chem. Soc. 112*, 2558−2566.
Norris, J. R., Thurnauer, M. C., & Bowman, M. K. (1980) *Adv. Biol. Med. Phys. 17*, 365−416.
Petrovich, R. M., Ruzicka, F. J., Reed, G. H., & Frey, P. A. (1991) *J. Biol. Chem. 266*, 7656−7660.
Rose, M. E. (1957) *Elementary Theory of Angular Momentum*, pp 49−52, John Wiley & Sons, New York.
Salowe, S., Bollinger, J. M., Jr., Ator, M., Stubbe, J., McCracken, J., Peisach, J., Samano, M. C., & Robins, M. J. (1993) *Biochemistry 32*, 12749−12760.
Stadtman, T. C. (1973) *Adv. Enzymol. Relat. Areas Mol. Biol. 38*, 413−448.
Stock, A., Ortanderl, F., & Pfliederer, G. (1966) *Biochem. Z. 344*, 353−360.
Tan, S. L., Kopezynski, M. G., Bachovchin, W. W., Orme-Johnson, W. H., & Babior, B. M. (1986) *J. Biol. Chem. 261*, 3483−3485.
Wada, H., & Snell, E. E. (1961) *J. Biol. Chem. 236*, 2089−2095.

BI951042G